Science Bulletin 64 (2019) 1567–1572

Contents lists available at ScienceDirect

Science Bulletin

journal homepage: www.elsevier.com/locate/scib

Short Communication

Metallic interface induced by electronic reconstruction in crystalline-amorphous bilayer oxide films

HPSTAR 888-2019

Xujie Lü [a,*], Aiping Chen [b], Yaomin Dai [c], Bin Wei [d], Hongwu Xu [e], Jianguo Wen [f], Nan Li [b], Yongkang Luo [g], Xiang Gao [a], Erik Enriquez [b], Zhongchang Wang [d], Paul Dowden [b], Wenge Yang [a], Yusheng Zhao [h], Quanxi Jia [i,j,*]

[a] Center for High Pressure Science and Technology Advanced Research (HPSTAR), Shanghai 201203, China
[b] Center for Integrated Nanotechnologies, Los Alamos National Laboratory, Los Alamos, NM 87545, USA
[c] Center for Superconducting Physics and Materials, National Laboratory of Solid State Microstructures and Department of Physics, Nanjing University, Nanjing 210093, China
[d] Department of Quantum Materials Science and Technology, International Iberian Nanotechnology Laboratory (INL), Av. Mestre José Veiga s/n, Braga 4715-330, Portugal
[e] Earth and Environmental Sciences Division, Los Alamos National Laboratory, Los Alamos, NM 87545, USA
[f] Center for Nanoscale Materials, Argonne National Laboratory, Lemont, IL 60439, USA
[g] Wuhan National High Magnetic Field Center and School of Physics, Huazhong University of Science and Technology, Wuhan 430074, China
[h] Department of Physics and Academy for Advanced Interdisciplinary Studies, Southern University of Science and Technology, Shenzhen 518055, China
[i] Department of Materials Design and Innovation, University at Buffalo, The State University of New York, Buffalo, NY 14260, USA
[j] Division of Quantum Phases and Devices, Department of Physics, Konkuk University, Seoul 143-701, Republic of Korea

ARTICLE INFO

Article history:
Received 12 June 2019
Received in revised form 13 July 2019
Accepted 8 August 2019
Available online 26 August 2019

© 2019 Science China Press. Published by Elsevier B.V. and Science China Press. All rights reserved.

Extraordinary electronic properties can emerge at the interfaces between metal oxides [1–10]. Interfacial behaviors have enabled a wide range of applications from electronic communication, energy conversion and storage, to data processing and memory. In recent years, unprecedented progress has been made in exploring and exploiting the emergent and/or enhanced properties of these interfaces, and it is becoming clear that interface engineering provides a new opportunity for advanced devices in the near future. The capability of using interfaces to manipulate material properties offers an effective means to achieve intriguing phenomena. Examples include the interfacial superconductivity in engineered oxide thin films [3,4,11,12], and a high-mobility electron (hole) gas at the interface between two insulating oxides such as $LaAlO_3$ (LAO) and $SrTiO_3$ (STO) [1,13–16]. The formation of highly conducting or even superconducting interfaces between two insulating materials opens a new route for the development of high-performance platforms such as transparent conducting oxide (TCO) films, which represents an ideal model system for electronic and optoelectronic applications [5].

Thus far, the interface-induced emergent properties are usually generated in heterostructures and depend highly on the interfacial chemistry and configuration, where precise control of surface terminations is indispensable [1,6,17]. For example, in the LAO/STO system, the conducting or insulating interface is determined by the surface termination of STO, that is, TiO_2-terminated STO brings a conducting interface while the SrO termination induces an insulating interface. More recently, we have illustrated an alternative and simpler system of bilayer TiO_2 thin film possessing a crystalline-amorphous homointerface [7], where the electronic properties were significantly modified and a conducting layer was formed by electronic reconstruction across the homointerface between the crystalline and amorphous TiO_2 layers. Nevertheless, it is still not clear whether such electronic reconstruction across the crystalline-amorphous homointerface is universal for binary oxides or limited to certain materials systems.

In this work, by using a series of characterization methods including transport measurements, terahertz spectroscopy, scanning transmission electron microscopy, and electron energy-loss spectroscopy, we present an insightful understanding of the electronically reconstructed interface and propose a strategy for realizing the highly conductive metallic interfaces in metal oxide films. More specifically, the metallic interface is induced by electronic reconstruction in crystalline-amorphous bilayer films of the oxides whose cations (metal ions) possess multiple valence states. In particular, tin oxide (SnO_2) bilayer film with such a crystalline-

* Corresponding authors.
E-mail addresses: xujie.lu@hpstar.ac.cn (X. Lü), qxjia@buffalo.edu (Q. Jia).

https://doi.org/10.1016/j.scib.2019.08.026
2095-9273/© 2019 Science China Press. Published by Elsevier B.V. and Science China Press. All rights reserved.

amorphous homointerface exhibits an electrical resistivity as low as $4.8 \times 10^{-4}\ \Omega$ cm (in comparison, the resistivities are 0.08 and 65 Ω cm for the single-layer crystalline and amorphous films, respectively) and an optical transmittance of ~90% in the visible-light region, showing great promise as an alternative to TCO films.

Bilayer SnO_2 thin films were prepared by growing an epitaxial SnO_2 layer on *M*-cut Al_2O_3 substrates at 700 °C using pulsed laser deposition (PLD), then deposited an amorphous layer at 100 °C on top of the epitaxial layer. Single-layer epitaxial and amorphous films were also prepared as reference samples. Further experimental details can be found in Table S1 (online). As shown in Fig. 1a, a peak assigned to rutile-type SnO_2 (0 0 2) ($P4_2/mnm$, $a = b = 4.738$ Å, $c = 3.187$ Å) is evident in the X-ray diffraction (XRD) patterns of the bilayer and single-layer epitaxial (or crystalline) films, indicating a preferred orientation along (0 0 1) of the films grown at 700 °C. By contrast, the single-layer film deposited at 100 °C does not have any SnO_2 diffraction peak, suggesting its amorphous nature. Fig. 1b shows the XRD Phi-scans of SnO_2 films and *M*-cut Al_2O_3 substrate. The four-fold symmetry of SnO_2 (1 0 1) planes, together with the XRD normal scan, confirms that the epitaxial relationship between the film and substrate is $SnO_2(0\,0\,2)||Al_2O_3(10\bar{1}0)$ and SnO_2 [0 0 1]||Al_2O_3 [0001].

Scanning transmission electron microscopy (STEM) was employed to examine the microstructure and interfacial configuration of the bilayer film. The cross-sectional STEM image in Fig. 1c shows that the thicknesses of the crystalline (i.e., epitaxial) and amorphous layers are 37 and 13 nm, respectively. As shown in Fig. 1d–f, high-angle annular dark field scanning transmission electron microscopy (HAADF-STEM) images confirm the high crystallinity of the bottom layer and the amorphous nature of the top layer, where the epitaxial growth and sharp interface between the sapphire substrate and crystalline SnO_2 layer can be clearly seen while the crystalline-amorphous interface is relatively rough. Selected-area electron diffraction (SAED) of the crystalline layer further confirms its high crystallinity and (0 0 1) oriented epitaxial growth (Fig. 1g).

The temperature-dependent electron transport properties of the SnO_2 films were evaluated by electrical resistivity (ρ_{xx}) and Hall resistivity (ρ_{yx}) measurements. As shown in Fig. 2a, the bilayer film exhibits dramatically different transport behavior from the single-layer ones (crystalline or amorphous). The room-temperature (RT) resistivity of the bilayer film is $4.8 \times 10^{-4}\ \Omega$ cm, which is several orders of magnitude smaller than those of the single-layer films. More interestingly, the bilayer SnO_2 film exhibits a metallic conducting behavior, whose resistivity decreases upon cooling from RT to 110 K. By contrast, both the single-layer films show insulating or semiconducting behavior with their resistivity increasing exponentially with decreasing temperature. In the bilayer film, possible origins of its high conductivity include (i) oxygen vacancies formed in the amorphous layer; (ii) electron transport at the interface between crystalline-SnO_2 layer and *M*-Al_2O_3 substrate; and (iii) interfacial electron transport between the crystalline and amorphous layers. The former two possibilities can be ruled out by comparing the temperature-dependent resistivities of these three types of films. That is, both the single-layer amorphous and crystalline films exhibit much higher resistivity and insulating *R-T* behavior, where oxygen vacancies also exist in the single-layer amorphous film and the crystalline film possesses the crystalline-SnO_2/*M*-Al_2O_3 interface. More detailed discussion on the interface-dominated conductivity can be seen in the Supplementary data (online). Further, in order to investigate whether such a metallic interface is orientation-dependent, the bilayer SnO_2 films deposit on various substrates of *R*- and *M*-cut Al_2O_3 as well as rutile TiO_2(0 0 1) were compared in Fig. S1 (online). These films clearly possess different orientations for the crystalline layer but exhibit the same metallic conduction behavior. Moreover, a bilayer film with doubled thicknesses for both crystalline and amorphous layers shows similar sheet resistances (Fig. S2 online), which confirms the interface-dominated conduction. Therefore, the metallic conduction in the bilayer SnO_2 film stems from the formation of a conducting sheet at the crystalline-amorphous interface. Note that the resistivity-temperature (ρ_{xx}-*T*) curve of the bilayer SnO_2 film

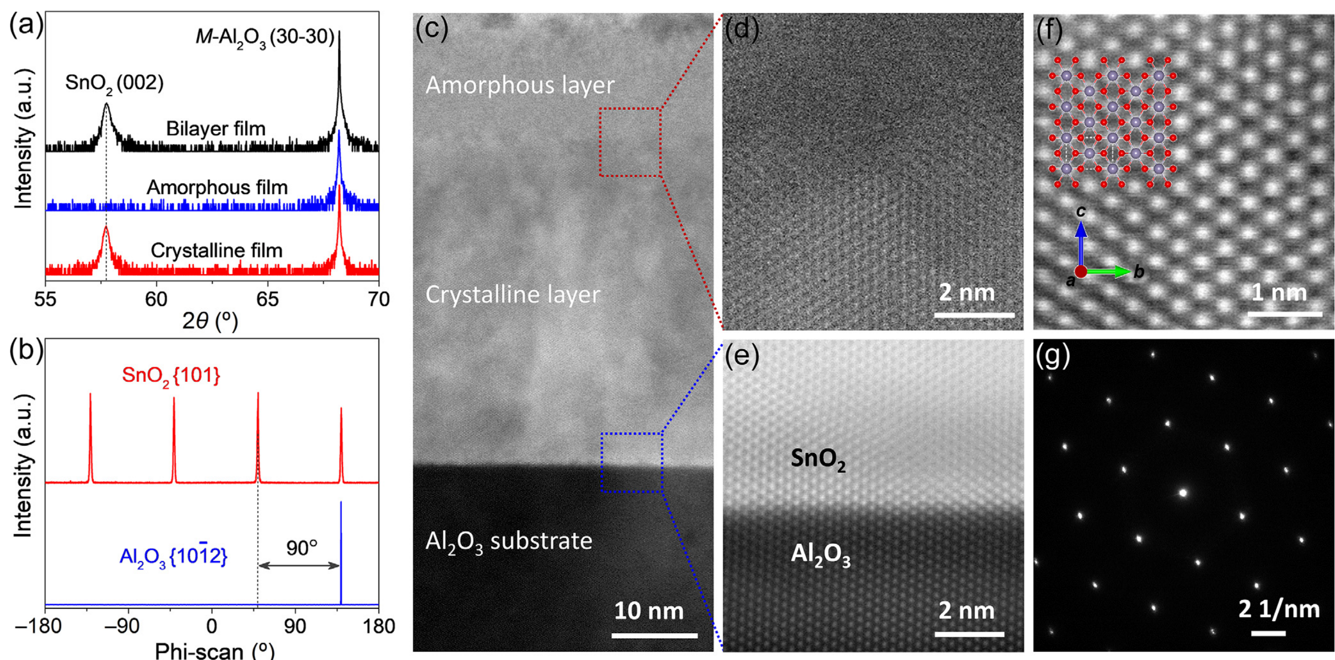

Fig. 1. Structural characterizations of the tin oxide films. (a) XRD 2θ-ω scans of the three types of SnO_2 films on *M*-cut Al_2O_3 single-crystal substrate. (b) Phi-scans for the (1 0 1) reflections of the SnO_2 films and $(10\bar{1}2)$ reflection of the *M*-cut Al_2O_3 substrate. (c) Cross-sectional TEM image of the bilayer film, which shows that the thicknesses of the crystalline (epitaxial) and amorphous layer are 37 and 13 nm, respectively. HAADF-STEM images of the crystalline-amorphous interface (d), substrate-crystalline interface (e), and the crystalline layer (f). The inset in (f) shows the crystal structure of SnO_2 in the corresponding orientation (Sn in purple and O in red). (g) SAED pattern of the crystalline SnO_2 layer.

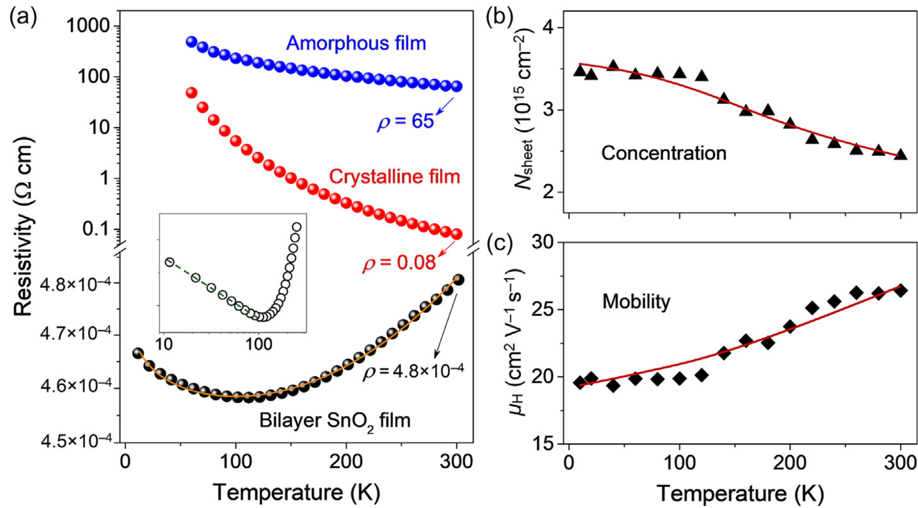

Fig. 2. Electrical properties of the three types of tin oxide films. (a) Resistivities of the bilayer film (black), the single-layer crystalline (red), and the amorphous (blue) films. The solid orange line is the fitted $\rho_{xx}(T)$ curve using a parallel conduction channel model. The inset shows the resistivity of the bilayer film plotted on a log$T$ scale. (b, c) Temperature-dependent sheet electron concentration (N_{sheet}) and Hall mobility (μ_H) of the bilayer film. The solid red lines are a guide to the eye.

exhibits an upturn below 110 K. Such an upward trend in resistivity cannot be interpreted in terms of the Arrhenius equation ($\rho_{xx} \propto$ exp (E_a/k_BT), where E_a is the activation energy and k_B is Boltzmann constant), but well agrees with the $-$log$T$ law (see the inset of Fig. 2a). This suggests that the increase in resistivity at low temperatures is probably caused by the electron localization due to disorder potentials, rather than the reduction of thermal activation energy [18].

Hall effect measurements were performed by scanning the magnetic fields at fixed temperatures down to 10 K. The Hall resistivity ρ_{yx} is linear with the magnetic field at each temperature and the Hall coefficient is negative, indicating electron-dominant conduction in the bilayer SnO_2 film. Fig. 2b, c displays the temperature dependence of the sheet carrier concentration (N_{sheet}) and Hall mobility (μ_H) of the bilayer film. The N_{sheet} and μ_H values at RT are $\sim 10^{15}$ cm^{-2} and 27 cm^2 V^{-1} s^{-1}, respectively. The N_{sheet} of the bilayer film decreases slightly with increasing temperature, which is apparently in contradiction with a typical semiconductor (or an insulator) in which the carrier concentration increases exponentially as temperature increases [18]. This further confirms the metallic conducting behavior of the bilayer film. By designing such a crystalline-amorphous interface, the electron transport properties of the bilayer oxide films are comparable to or even better than the values obtained in the TCO films via ion doping (Table S2 online). Therefore, both high carrier concentration and high mobility are achieved concurrently in the oxide films by constructing a crystalline-amorphous homointerface.

The metallic character of the bilayer SnO_2 film was further confirmed by its optical conductivity, which was measured using time-domain terahertz (THz) spectroscopy (Fig. S3 online). Optical conductivity is sensitive to the presence of metallic conduction, with its zero-frequency extrapolation being the direct-current conductivity which exhibits a Drude response in the low-frequency range [19]. As shown in Fig. 3, a pronounced Drude response is shown for the bilayer film, which was fitted by the Drude model.

$$\sigma_1(\omega) = \frac{2\pi}{Z_0}\frac{\Omega_p^2}{\tau(\omega^2+\tau^{-2})}, \tag{1}$$

where σ_1 is the optical conductivity, Z_0 is the vacuum impedance ($\approx$377 Ω), ω is the photon energy, Ω_p and $1/\tau$ correspond to the plasma frequency and scattering rate of the free carriers, respectively. The low-frequency Drude response of the bilayer film clearly indicates its metallic conduction. The zero-frequency value of the

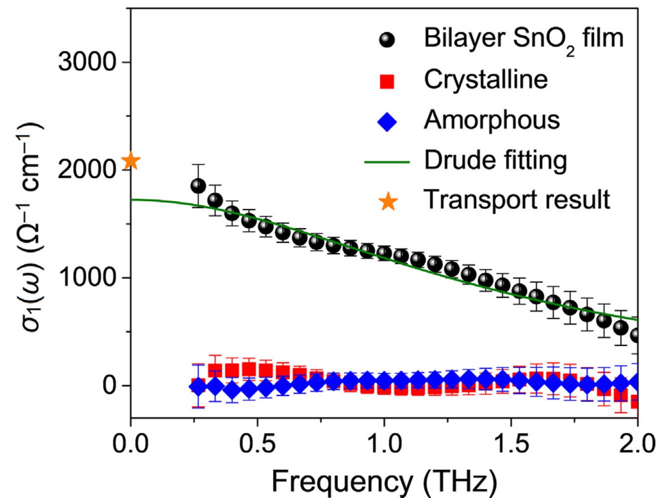

Fig. 3. THz optical conductivities of SnO_2 bilayer (sphere), crystalline (square) and amorphous (diamond) films at RT. The solid line is a Drude fit to the data of the bilayer film, which gives a reasonably good description of the experimental data. The star symbol at zero frequency represents the conductivity value obtained from transport measurement.

Drude fit is in line with the result from the transport measurement (shown as a star in Fig. 3), whose values are 1725 and 2083 Ω^{-1} cm^{-1}, respectively. In contrast, the optical conductivities of the single-layer films are significantly smaller and frequency independent, which suggest their non-metallic transport behavior.

We have demonstrated interface-induced metallic conduction in bilayer SnO_2 thin films. Such an intriguing phenomenon motivated us to uncover its underlying mechanisms. In the bilayer film, oxygen vacancies form in the amorphous layer due to the low-oxygen pressure (10^{-6} Torr) during film growth. Meanwhile, Sn has accessible mixed-valence states of Sn^{4+} and Sn^{2+}. In order to maintain the charge neutrality, the formation of one oxygen vacancy needs to be accompanied by the reduction of one Sn^{4+} ion to Sn^{2+}, yielding $Sn_x^{2+}Sn_{(1-x)}^{4+}O_{2-x}$. Two extra electrons, which occupy the conduction band (CB) orbital in each Sn^{2+}, are transferable and could migrate across the interface when energetically favorable. Defects in the amorphous layer (such as oxygen vacancies and disorders) could result in the formation of a narrow band

of states close to the bottom of CB where the Fermi level (E_F) is pinned [18,20]. Thus, E_F in the amorphous layer is closer to CB than it is in the highly crystalline layer. On the other hand, the highly crystallized layer ensures low defect content, leading to a low carrier concentration but a relatively high mobility. Once the amorphous layer is stacked on the crystalline layer, electrons transfer from the amorphous layer to the crystalline surface to balance their chemical potentials, as schematically illustrated in Fig. 4a. The transferred electrons would be confined in the near-interface region of the crystalline layer due to the built-in potential [13]. We would like to point out that these electrons distribute inhomogeneously at the interfacial region, as evidenced by the upturn of the resistivity-temperature curve below 110 K. Such an upward trend can be interpreted by the –log$T$ law (see the inset of Fig. 2a), which suggests that the increase in resistivity at low temperatures is due to electron localization [18]. Experimentally, the microscopic distribution of Sn valence states at the interface was probed by electron energy loss spectroscopy (EELS). Despite the substantial overlap between the O-K and Sn-$M_{4,5}$ edges, it is still possible to distinguish the oxidation states of Sn^{4+} and Sn^{2+} using EELS where the oxygen edges exhibit different configurations [21,22]. Specifically, the Sn^{4+} state corresponds to a O-K fine structure with peak separation of about 6 eV, whereas the Sn^{2+} state contributes to an obviously narrower energy interval. EELS spectra collected at the interface, 0.5, 1.0, 2.0, 3.0, and 4.0 nm away from the interface as well as the standard EELS spectra for pure SnO_2 and SnO are displayed in Fig. 4b, which indicates the existence of Sn^{2+} in the amorphous layer, at the interface, and in the crystalline layer close to the interface within about 2 nm (see more details in Supplementary data online). Consequently, the confined electrons in the near-interface region give rise to a high carrier concentration, as reflected by the transport measurements shown in Fig. 2. These interfacial electrons are compensated by the reduced Sn^{2+} that places the two electrons into the CB orbitals of crystalline SnO_2. The electron mean free path l is determined to be 20 nm (see details in Supplementary data online), which is an order of magnitude larger than the interfacial thickness. This suggested that although the crystalline-amorphous interface is relatively rough, the transferred electrons can be well confined in a thin region (~2 nm) where the metallic sheet forms. Therefore, the electronic reconstruction occurs by the electron transfer, forming the quasi two-dimensional electron gas (quasi-2DEG) at the interface [1,23,24].

The electronically reconstructed interface has been demonstrated in the SnO_2 bilayer film as well as in the TiO_2 system we studied earlier [7]. The next question is whether such an electronic reconstruction at the crystalline-amorphous interface of oxides is universal or unique to certain systems. Unlike conventional semiconductors where each ion has a fixed valence, metal oxides have another option for charge rearrangement in addition to compositional compensation [2,25]. That is, mixed-valence charge compensation occurs if electron redistribution is energetically more favorable than the redistribution of ions such as oxygen vacancy. Here, we propose that interfacial electronic reconstruction exists in the crystalline-amorphous bilayer films of oxides whose cations (metal ions) possess multiple valence states. For both SnO_2 and TiO_2, the metal ions have two different valence states (+2 & +4 for Sn, and +3 & +4 for Ti). Mixed-valence charge compensation is favorable for charge rearrangement since the energy required to change the valence is usually small in the oxides whose metal ions adopt multiple-valence states [26]. Hence, electronic reconstruction can be achieved in these multiple-valence metal oxides, resulting in both high electron concentration and high mobility at the crystalline-amorphous interface. In this case, instead of the polar discontinuity in LAO/STO heterostructures, mixed-valence charge rearrangement at the interface induces the electronic reconstruction.

For comparison, we constructed the crystalline-amorphous bilayer film for an oxide without multiple oxidation states, zinc oxide (ZnO), in which only +2 valence is accessible for the Zn ion. ZnO films (bilayer, single-layer crystalline and amorphous) were deposited using PLD, and the experimental details and XRD patterns are shown in Table S3 (online) and Fig. 4c, respectively. In contrast to SnO_2, ZnO bilayer film exhibits semiconductive

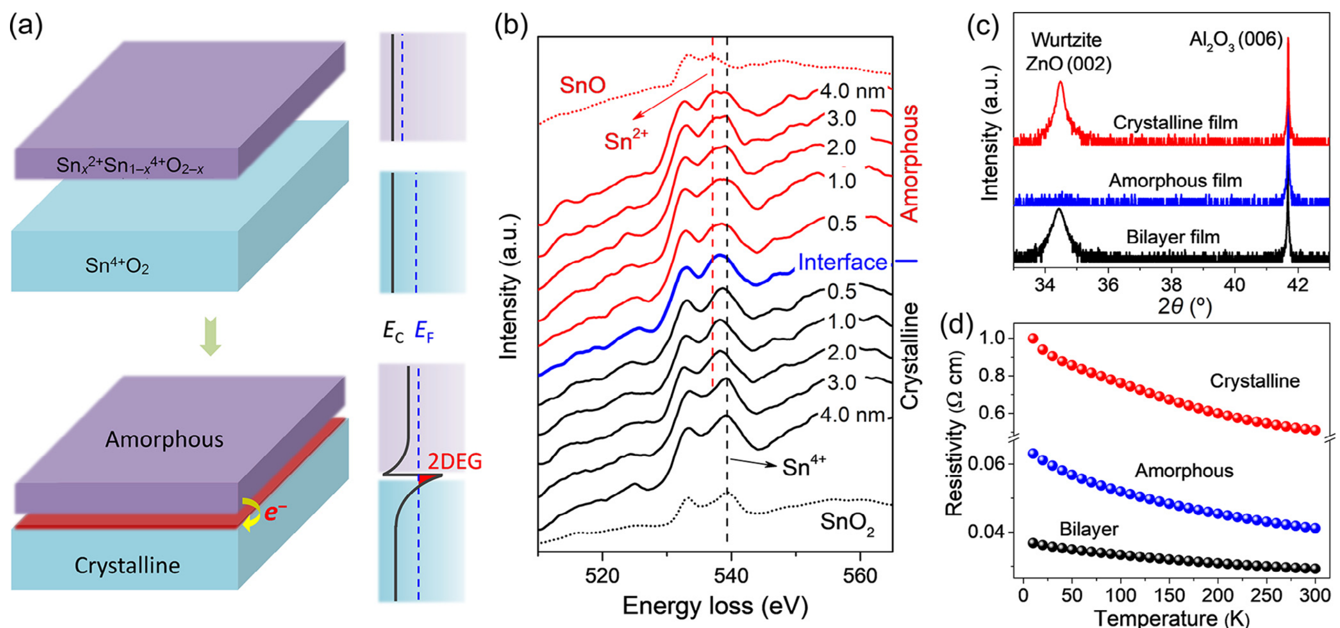

Fig. 4. (Color online) Origin of the metallic conduction at the homointerface. (a) Schematic illustrations of the crystalline-amorphous interface structure (left panel) and the corresponding schematic of the band diagram (right panel) before and after reconstruction, where electrons transfer from the top amorphous layer to the bottom crystalline layer, achieving electronic reconstruction and creating the quasi-2DEG. E_C and E_F are the conduction-band-edge and Fermi-level energies, respectively. (b) Selected O-K EELS spectra recorded at various positions near the crystalline-amorphous interface, which indicates the existence of Sn^{2+} in the amorphous layer, at the interface, and in the crystalline side close to the interface (within about 2 nm). The top and bottom dot lines are the EELS spectra for pure SnO and SnO_2, respectively. XRD patterns (c) and temperature-dependent resistivity (d) of the ZnO bilayer films, single-layer crystalline and amorphous films.

behavior in which the resistance increases with decreasing temperature, similar to the single-layer crystalline and amorphous films (Fig. 4d). In this situation, compositional compensation (such as the formation of oxygen vacancies) is the only option for charge rearrangement at the interface of bilayer ZnO film, and electronic reconstruction would not happen. Oxygen vacancies, diffusing from the amorphous to crystalline layer at the interface, play a dominant role in determining the electrical conductivity, but no substantial changes in the electronic properties can be achieved. This further confirms that the interfacial electronic reconstruction instead of the interfacial oxygen vacancy diffusion is responsible for the formation of metallic interface. Particularly, in comparison to the single-layer crystalline or amorphous film, SnO_2 bilayer film exhibits significantly enhanced conductivity by several orders of magnitude via electronic reconstruction, whereas the ZnO bilayer film shows only a small improvement via the diffusion of oxygen vacancies at the interface.

Most metal oxides are insulators or semiconductors when they are perfectly stoichiometric. Once their composition deviates from stoichiometry, which results in an excess or deficiency of the metal or oxygen ions, the materials show increased conductivity due to the increased carrier concentration. However, carrier mobility usually decreases with increasing carrier concentration because the defects (such as oxygen vacancies) act as charge trapping and scattering centers. This is why the single-layer amorphous film of tin oxide cannot realize the high conductivity by itself. Alternatively, by engineering the interface, electronic reconstruction happens in the crystalline-amorphous bilayer films of the oxides whose metal ions possess multiple valences. Consequently, the near-interface region offers dual functionalities: high electron concentration provided by the amorphous layer and high electron mobility supplied by the crystalline layer. The reconstructed interface, as such, acts as the highway for electron transport. Therefore, such an interfacial engineering strategy concurrently enables high carrier concentration and high mobility in the oxide films to achieve superior conductivity.

In addition to the electron transport property, optical transparency is another key parameter for optoelectronic applications. The bilayer SnO_2 thin film exhibits a high internal transmittance of $\sim$90% in the visible-light region (Fig. S4 online). Hence, interfacial engineering of oxide bilayer films based on electronic interface reconstruction can successfully promote electron transport without significantly affecting transparency. It opens a new way for exploring novel highly conducting oxide films and devices by constructing crystalline-amorphous homointerfaces. The interfacially engineered bilayer films possess prominent electronic and optical properties, rendering these materials promising for various applications including high-performance light-emitting diodes and high-efficient photovoltaic devices.

In summary, we report the emergent property of metallic conduction forming at the crystalline-amorphous interface in bilayer oxide films via interfacial electronic reconstruction. By employing a series of characterization methods, we demonstrated that the electronic-reconstruction-induced metallic interfaces are unique to the oxide systems whose metal ions possess multiple valence states such as tin and titanium. In particular, SnO_2 bilayer film with such a crystalline-amorphous interface exhibits an electrical resistivity as low as $4.8 \times 10^{-4}\ \Omega$ cm and optical transmittance of $\sim$90% in the visible-light region, showing great promise for optoelectronic applications. Our findings not only provide a strategy for realizing highly conductive metallic interfaces in oxide films, but also achieve an unprecedented understanding of the underlying mechanisms of the electronically reconstructed interfaces in the oxide homostructures. That is, in addition to the polar discontinuity at the hetero-epitaxial $LaAlO_3/SrTiO_3$ interface, mixed-valence charge rearrangement across the homointerfaces would be another chance for the interfacial electronic reconstruction. Since the exploration and understanding of the engineered interfaces in oxides are just emerging, more novel phenomena are expected to be uncovered by carefully designing the interfaces and optimizing the growth conditions.

Conflict of interest

The authors declare that they have no conflict of interest.

Acknowledgments

This work was supported by the National Nature Science Foundation of China (U1530402, 17N1041). A. C. acknowledges the support from the NNSA's Laboratory Directed Research and Development Program, where the work was performed, in part, at the Center for Integrated Nanotechnologies (CINT), an Office of Science User Facility operated for the U.S. Department of Energy Office of Science. Q. X. J. acknowledges the CINT User Program and the support by the U. S. National Science Foundation (ECCS-1902623). Z. W. acknowledges the support by the National Nature Science Foundation of China (51728202), the Center for Nanoscale Materials, an Office of Science user facility, supported by the U.S. Department of Energy (DE-AC02-06CH11357). X. Lü thanks Shan Guo and Aiden Lü for their great support. The authors appreciate the language editing by Editor Freyja O'Toole.

Author contributions

Xujie Lü and Quanxi Jia managed the project, initiated the research, and designed the experiments. Xujie Lü, Aiping Chen, and Paul Dowden deposited the films; Aiping Chen and Erik Enriquez conducted the XRD measurements. Xujie Lü, Aiping Chen, and Yongkang Luo conducted the transport measurements. Yaomin Dai measured the optical conductivity using terahertz spectroscopy. Bin Wei, Jianguo Wen, Nan Li, Xiang Gao, and Zhongchang Wang performed the TEM and EELS measurements. Hongwu Xu, Wenge Yang, and Yusheng Zhao involved in the discussion and manuscript drafting. Xujie Lü, Hongwu Xu, and Quanxi Jia wrote the manuscript, and all authors have approved the final version of the manuscript.

Appendix A. Supplementary data

Supplementary data to this article can be found online at https://doi.org/10.1016/j.scib.2019.08.026.

References

[1] Ohtomo A, Hwang HY. A high-mobility electron gas at the $LaAlO_3/SrTiO_3$ heterointerface. Nature 2004;427:423–6.
[2] Nakagawa N, Hwang HY, Muller DA. Why some interfaces cannot be sharp. Nat Mater 2006;5:204–9.
[3] Reyren N, Thiel S, Caviglia AD, et al. Superconducting interfaces between insulating oxides. Science 2007;317:1196–9.
[4] Gozar A, Logvenov G, Kourkoutis LF, et al. High-temperature interface superconductivity between metallic and insulating copper oxides. Nature 2008;455:782–5.
[5] Mannhart J, Schlom D. Oxide interfaces—an opportunity for electronics. Science 2010;327:1607–11.
[6] Hwang HY, Iwasa Y, Kawasaki M, et al. Emergent phenomena at oxide interfaces. Nat Mater 2012;11:103–13.
[7] Lü X, Chen A, Luo Y, et al. Conducting interface in oxide homojunction: understanding of superior properties in black TiO_2. Nano Lett 2016;16:5751–5.
[8] Frano A, Blanco-Canosa S, Schierle E, et al. Long-range charge-density-wave proximity effect at cuprate/manganate interfaces. Nat Mater 2016;15:831–4.
[9] Ohshima R, Ando Y, Matsuzaki K, et al. Strong evidence for d-electron spin transport at room temperature at a $LaAlO_3/SrTiO_3$ interface. Nat Mater 2017;16:609–14.
[10] Kim SM, Kim HJ, Jung HJ, et al. High-performance, transparent thin film hydrogen gas sensor using 2D electron gas at interface of oxide thin film

heterostructure grown by atomic layer deposition. Adv Funct Mater 2019;29:1807760.
[11] Stornaiuolo D, Cantoni C, De Luca GM, et al. Tunable spin polarization and superconductivity in engineered oxide interfaces. Nat Mater 2016;15:278–83.
[12] Goswami S, Mulazimoglu E, Monteiro AMRVL, et al. Quantum interference in an interfacial superconductor. Nat Nanotechnol 2016;11:861–5.
[13] Singh-Bhalla G, Bell C, Ravichandran J, et al. Built-in and induced polarization across $LaAlO_3$/$SrTiO_3$ heterojunctions. Nat Phys 2011;7:80–6.
[14] Chen YZ, Trier F, Wijnands T, et al. Extreme mobility enhancement of two-dimensional electron gases at oxide interfaces by charge-transfer-induced modulation doping. Nat Mater 2015;14:801–6.
[15] Lee PW, Singh VN, Guo GY, et al. Hidden lattice instabilities as origin of the conductive interface between insulating $LaAlO_3$ and $SrTiO_3$. Nat Commun 2016;7:12773.
[16] Lee H, Campbell N, Lee J, et al. Direct observation of a two-dimensional hole gas at oxide interfaces. Nat Mater 2018;17:231–6.
[17] Minohara M, Tachikawa T, Nakanishi Y, et al. Atomically engineered metal-insulator transition at the TiO_2/$LaAlO_3$ heterointerface. Nano Lett 2014;14:6743–6.
[18] Ashcroft NW, Mermin ND. Solid state physics. New York: Harcourt College Publisher; 1976.
[19] Dressel M, Grüner G. Electrodynamics of solids: optical properties of electrons in matter. Cambridge: Cambridge University Press; 2002.
[20] Ovshinsky SR. Disordered materials: science and technology. Berlin: Springer Science & Business Media; 2012.
[21] Moreno MS, Egerton RF, Midgley PA. Differentiation of tin oxides using electron energy-loss spectroscopy. Phys Rev B 2004;69:233304.
[22] Moreno MS, Egerton RF, Rehr JJ, et al. Electronic structure of tin oxides by electron energy loss spectroscopy and real-space multiple scattering calculations. Phys Rev B 2005;71:035103.
[23] Cantoni C, Gazquez J, Miletto Granozio F, et al. Electron transfer and ionic displacements at the origin of the 2D electron gas at the LAO/STO interface: direct measurements with atomic-column spatial resolution. Adv Mater 2012;24:3952–7.
[24] Chen Y, Pryds N. 2D hole gas seen. Nat Mater 2018;17:215–6.
[25] Enriquez E, Chen A, Harrell Z, et al. Oxygen vacancy-tuned physical properties in perovskite thin films with multiple B-site valance states. Sci Rep 2017;7:46184.
[26] Johnston WD. Mixed valence oxides. J Chem Educ 1959;36:605.

Xujie Lü is currently a staff scientist at the Center for High Pressure Science & Technology Advanced Research (HPSTAR). He received his Bachelor's degree from Zhejiang University at 2006, and his Ph.D. degree from Shanghai Institute of Ceramics, Chinese Academy of Sciences at 2011. He was the J. Robert Oppenheimer Distinguished Fellow in Los Alamos National Laboratory before joining in HPSTAR at 2017. His research focuses on the optoelectronic materials, *in-situ* characterization under extreme environments, and multifunctional oxide thin films.

Quanxi Jia is an Empire Innovation Professor and National Grid Professor of Materials Research at the University at Buffalo (UB) – the State University of New York. Prior to joining UB in 2016, he had worked at Los Alamos National Laboratory for 24 years, with the last two years serving as the co-Director and then Director of the Center for Integrated Nanotechnologies, a US Department of Energy Nanoscale Science Research Center operated jointly by Los Alamos and Sandia National Laboratories. His research focuses on nanostructured and multifunctional materials, with a particular effort on the synthesis and study of processing-structure–property relationships of epitaxial films for energy and electronic applications.